# Novel Ionic Liquid-Crystalline Compounds Bearing Oxadiazole and Pyridinium Moieties as Prospective Materials for Optoelectronic Applications

Denis Haristoy* and Dimitris Tsiourvas

*Institute of Physical Chemistry, NCSR "Demokritos", Aghia Paraskevi, Attiki, Greece*

*Received November 28, 2002. Revised Manuscript Received March 10, 2003*

Novel liquid-crystal materials based on 1-alkyl-4-[5-(dodecylsulfanyl)-1,3,4-oxadiazol-2-yl]pyridinium bromide derivatives were synthesized. Their thermotropic polymorphism was investigated by polarizing optical microscopy and differential scanning calorimetry. The structures of their crystalline and smectic A phases were investigated by X-ray diffraction. The existence of thermochromic properties in the smectic phase as well as their UV−visible and fluorescence properties were also studied. The chemical structure of the compounds renders these materials suitable for optoelectronic applications.

## Introduction

Functional organic materials with optical and electronic properties have recently been intensively investigated.[1] These materials should be designed in such a manner as to permit control of the molecular organization and exhibit excellent processability, transparency, and absence of grain boundaries. Liquid-crystalline materials are meeting these needs since they present self-organizing ability, fluidity, and ease of defect-free orientation on specially treated surfaces. The influence of the molecular order induced by mesophases has been clearly established for several properties including magnetic,[2] nonlinear optical generation,[3] conduction,[4] photoconduction,[5−8] and electroluminescence.[9,10]

At present, most of the organic compounds known for optoelectronic applications still present some major limitations such as low electron conductivity or luminescence efficiency. Indeed, the great majority of organic compounds are better known as hole conductors since they donate more easily electrons than they can accept. One of the easiest ways to bypass this limitation is to introduce an electron acceptor group such as the oxadiazole,[9,11] the quinoline,[12] or the benzobisthiazole[13] moieties.

**Scheme 1. Chemical Structure of the 1-Alkyl-4-[5-(dodecylsulfanyl)-1,3,4-oxadiazol-2-yl]-pyridinium Bromide Derivatives (with $n$ = 10, 12, 14, 16)**

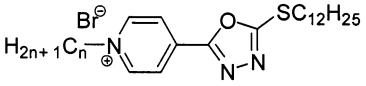


To obtain liquid-crystalline properties, the oxadiazole has been associated with an alkyl pyridinium ring. The electronic properties of this type of heteroaromatic ring have not, to the best of our knowledge, been clearly established. However, it is known that it is easily and reversibly reduced from a positively charged species to a free radical;[14] it could therefore exhibit some interesting electron transport property.

In this study a series of ionic liquid-crystalline compounds bearing both the oxadiazole and pyridinium groups were prepared (see Scheme 1). The coupling of these two moieties in an ionic compound would, in principle, enhance both its electron transport and conductivity. Their mesomorphic properties, some of their physicochemical properties such as UV and fluorescence, and their thermochromic properties were investigated.

## Experimental Section

**1. Materials and Synthesis.** The chemicals were purchased pure from Aldrich and used as received.

*Synthesis of 2-dodecylsulfanyl-5-(4-pyridinyl)-1,3,4-oxadiazole (**I**).* 5-(4-Pyridinyl)-1,3,4-oxadiazol-2-ylhydrosulfide, 1-bromododecane (1.2 equiv), and potassium hydroxide (1.5 equiv) were dispersed in a minimum quantity of ethanol. The suspension obtained was refluxed for 2 h. The ethanol was evaporated under reduced pressure and the solid obtained was dissolved in 100 mL of diethyl ether and washed with 100 mL of water. The organic phase was dried over $Na_2SO_4$, and the

* To whom correspondence should be addressed. Tel: +30210-6503616; +30210-6503638. Fax: +30210-6529792. E-mail: haristoy@chem.demokritos.gr.

(1) Nalwa, H. S. *Handbook of Conductive Molecules and Polymers*; John Wiley & Son Ltd.: New York, 1997.
(2) Belarbi, Z.; Sirlin, C.; Simon, J.; Andre, J. J. *J. Phys. Chem.* **1989**, *93*, 8105.
(3) Walba, D. M.; Blanca Ros, M.; Clark, N. A.; Shao, R.; Robinson, M. G.; Liu, J.-Y.; Johnson, K. M.; Doroski, D. *J. Am. Chem. Soc.* **1991**, *113*, 5471.
(4) Dias, F. B.; Batty, S. V.; Ungar, G.; Voss, J. P.; Wright, P. V. *J. Chem. Soc.* **1996**, *92*, 2599.
(5) Funahashi, M.; Hanna, J.-I. *Appl. Phys. Lett.* **1997**, *71*, 602.
(6) Méry, S.; Haristoy, D.; Nicoud, J.-F.; Guillon, D.; Diele, S.; Monobe, H.; Shimizu, Y. *J. Mater. Chem.* **2002**, *12*, 37.
(7) Funahashi, M.; Hanna, J.-I. *Appl. Phys. Lett.* **1998**, *73*, 3733.
(8) Funahashi, M.; Hanna, J.-I. *Appl. Phys. Lett.* **2000**, *76*, 2574.
(9) Tokuhisa, H.; Era, M.; Tsutsui, T. *Appl. Phys. Lett.* **1998**, *72*, 2639.
(10) Kogo, K.; Goda, T.; Funahashi, M.; Hanna, J.-I. *Appl. Phys. Lett.* **1998**, *73*, 1595.
(11) Peng, Z.; Zhang, J. *Chem. Mater.* **1999**, *11*, 1138.
(12) Zhang, X.; Jenekhe, S. A. *Macromolecules* **2000**, *33*, 2069.
(13) Alam, M. M.; Jenekhe, S. A. *Chem. Mater.* **2002**, *14*, 4775.
(14) Bird, C. L.; Kuhn, A. T. *Chem. Soc. Rev.* **1981**, *10*, 49.

10.1021/cm021365g CCC: $25.00 
Published on Web 04/12/2003

**Scheme 2. Synthesis of 1-Alkyl-4-[5-(dodecylsulfanyl)-1,3,4-oxadiazol-2-yl]pyridinium Bromide Derivatives: (i) $C_{12}H_{25}Br$, KOH, Ethanol, Reflux, 2 h; (ii) RBr, NaI, Acetonitrile, Reflux, 24 h**

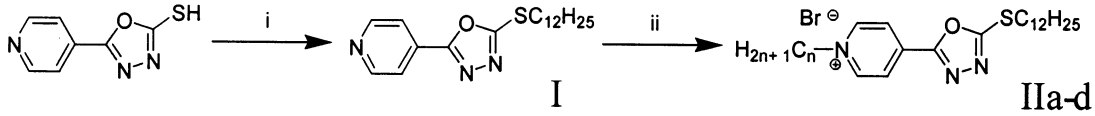


solvent distilled off under reduced pressure. The solid obtained was recrystallized first from ethanol and then from hexane, affording a white solid (40% average yield).

mp: 64.0−64.5 °C. $^1$H NMR ($CDCl_3$/250 MHz): 8.8 (dd, 4.5 + 1.5 Hz; 2 H), 7.8 (dd, 4.5 + 1.5 Hz; 2 H), 3.3 (t, 7.2 Hz; 2 H), 1.8 (q, 7.4 Hz; 2 H), 1.5 (q, 7.2 Hz; 2 H), 1.3 (m; 16 H), 0.9 (t, 6.5 Hz; 3 H). $^{13}$C NMR ($CDCl_3$/250 MHz): 166.3, 163.8, 150.9, 130.8, 120.0, 32.6, 31.9, 29.6, 29.5, 29.4, 29.3, 29.1, 29.0, 28.6, 22.7, 14.0. UV (solution in $CHCl_3$, nm): 282 ($14.6 \times 10^6$).

*Synthesis of 1-Alkyl-4-[5-(dodecylsulfanyl)-1,3,4-oxadiazol-2-yl]pyridinium Bromide (**II**).* 2-Dodecylsulfanyl-5-(4-pyridinyl)-1,3,4-oxadiazole and the appropriate 1-alkylbromine (1.1 equiv) were dissolved in acetonitrile and refluxed for 24 h. The reaction mixture was then slightly concentrated under reduced pressure and precipitated with 100 mL of hexane. The precipitated material was filtered off, dried under vacuum, dissolved in a small quantity of ethanol, reprecipitated with 100 mL of diethyl ether, filtered off, and dried under vacuum to give the pure pyridinium bromide derivative (30% average yield). This reaction has also been performed under similar conditions but with the addition of NaI (0.02 equiv), giving an average yield of 60%.

The structures of the compounds prepared were established by $^1$H NMR, $^{13}$C NMR, and elemental analysis. The $^1$H NMR peak corresponding to the methyl in the α position in regard to the sulfur atom (3.4 ppm) appeared too close to the peak of the water (3.6 ppm) to permit its integration in the case of the dodecyl, tetradecyl, and hexadecyl derivatives. In the case of the decyl derivative, the peak was completely overlapped by the peak of water and did not appear at all. The $^{13}$C NMR peaks of the pyridinium bromide derivatives are in agreement with the data published in the literature.[15]

*1-Decyl-4-[5-(dodecylsulfanyl)-1,3,4-oxadiazol-2-yl]pyridinium Bromide (**IIa**).* $^1$H NMR (DMSO/250 MHz): 9.2 (d, 6.8 Hz; 2 H), 8.6 (d, 6.8 Hz; 2 H), 4.6 (t, 7.3 Hz; 2 H), 1.9 (m, 2 H), 1.8 (m; 2 H), 1.4 (m; 2 H), 1.2 (m; 30 H), 0.8 (t, 6.5 Hz; 6 H). Anal. Calcd for $C_{29}H_{50}BrN_3OS \cdot H_2O$: C, 59.37; H, 8.93; Br, 13.62; N, 7.16; S, 5.47. Anal. Found for $C_{29}H_{50}BrN_3OS$: C, 59.84; H, 8.76; Br, 13.39; N, 7.25; S, 5.72.

*1-Dodecyl-4-[5-(dodecylsulfanyl)-1,3,4-oxadiazol-2-yl]pyridinium Bromide (**IIb**).* $^1$H NMR (DMSO/250 MHz): 9.2 (d, 6.8 Hz; 2 H), 8.6 (d, 6.6 Hz; 2 H), 4.6 (t, 7.5 Hz; 2 H), 3.4 (t, 7.3 Hz), 1.9 (m, 2 H), 1.8 (q, 6.7 Hz; 2 H), 1.4 (q, 7.1 Hz; 2 H), 1.3 (m; 34 H), 0.8 (t, 6.6 Hz; 6 H). $^{13}$C NMR ($CDCl_3$/250 MHz): 161.8, 146.0, 137.0, 124.2, 61.1, 32.2, 31.2, 30.6, 28.9, 28.8, 28.7, 28.6, 28.3, 27.7, 25.3, 22.0, 13.9. UV (solution in $CHCl_3$, nm): 236 ($12.5 \times 10^6$), 272 ($3.7 \times 10^6$), 278 ($3.9 \times 10^6$), 288 ($3.6 \times 10^6$), 347 ($16.5 \times 10^6$). Anal. Calcd for $C_{31}H_{54}BrN_3OS$: C, 62.39; H, 9.12; Br, 13.39; N, 7.04; S, 5.37. Anal. Found for $C_{31}H_{54}BrN_3OS$: C, 62.00; H, 9.19; Br, 13.32; N, 7.02; S, 5.60.

*1-Tetradecyl-4-[5-(dodecylsulfanyl)-1,3,4-oxadiazol-2-yl]pyridinium Bromide (**IIc**).* $^1$H NMR (DMSO/250 MHz): 9.2 (d, 6.6 Hz; 2 H), 8.6 (d, 6.6 Hz; 2 H), 4.6 (t, 7.3 Hz; 2 H), 3.4 (t, 7.6 Hz), 1.9 (m, 2 H), 1.8 (q, 7.3 Hz; 2 H), 1.4 (m; 2 H), 1.2 (m; 38 H), 0.8 (t, 7.3 Hz; 6 H). Anal. Calcd for $C_{33}H_{58}BrN_3OS \cdot H_2O$: C, 61.66; H, 9.3; Br, 12.49; N, 6.49; S, 5.09. Anal. Found for $C_{33}H_{58}BrN_3OS$: C, 61.66; H, 9.41; Br, 12.43; N, 6.54; S, 4.99.

*1-Hexadecyl-4-[5-(dodecylsulfanyl)-1,3,4-oxadiazol-2-yl]pyridinium Bromide (**IId**).* $^1$H NMR (DMSO/250 MHz): 9.2 (d, 6.8 Hz; 2 H), 8.6 (d, 6.8 Hz; 2 H), 4.6 (t, 7.3 Hz; 2 H), 3.4 (t, 7.3 Hz), 1.9 (m, 2 H), 1.8 (q, 7.4 Hz; 2 H), 1.4 (m; 2 H), 1.2 (m; 42 H), 0.8 (t, 6.4 Hz; 6 H). Anal. Calcd for $C_{35}H_{62}BrN_3OS$: C, 64.39; H, 9.57; Br, 12.24; N, 6.44; S, 4.91. Anal. Found for $C_{35}H_{62}BrN_3OS$: C, 64.15; H, 9.70; Br, 12.03; N, 6.44; S, 5.16.

(15) Bentiss, F.; Lagrenée, M. *J. Heterocycl. Chem.* **1999**, *36*, 1029.

**2. Characterization.** The thermal stability was assessed by thermogravimetry employing a TGA 2050 analyzer (TA instruments) at a heating rate of 10 °C min$^{-1}$. UV−visible spectra were recorded on a Perkin-Elmer Lambda-16 spectrophotometer and fluorescence spectra on a Perkin-Elmer LS-5B spectrophotometer. Elemental analyses were performed by the Service Central d'Analyse of CNRS (Vernaison-France).

Liquid-crystal textures were observed using a Leitz-Wetzlar polarizing microscope equipped with a Linkam hot-stage. Thermotropic polymorphism was investigated by differential scanning calorimetry employing a DSC-10 calorimeter (TA instruments) at heating/cooling rates of 10 °C min$^{-1}$. Liquid-crystalline phases were investigated by X-ray diffraction using Cu $K\alpha_1$ radiation from a Rigaku rotating anode X-ray generator (operating at 50 kV, 100 mA) and an R-AXIS IV image plate. Powder samples were sealed in Lindemann capillaries and heated employing an INSTEC hot-stage.

## Results and Discussion

**1. Synthesis of the Materials.** 1-Alkyl-4-[5-(dodecylsulfanyl)-1,3,4-oxadiazol-2-yl]pyridinium bromide derivatives have been prepared in two steps (see Scheme 2) from commercially available 5-(4-pyridinyl)-1,3,4-oxadiazol-2-ylhydro-sulfide. The sulfide group has been converted into a thioether by reaction with dodecylbromide under basic conditions to give the 2-dodecylsulfanyl-5-(4-pyridinyl)-1,3,4-oxadiazole (**I**). Reaction of pyridine moiety with the appropriate alkyl bromide in acetonitrile afforded the pyridinium derivatives (**IIa**−**d**).

The preparation of the pyridinium bromide derivatives was also performed in the presence of NaI (0.02 equiv). Under these conditions, the yield was increased to an average value of 60%. Indeed, it is well-established that some iodide compounds such as NaI or $NBu_4I$ promote quaternization reactions of heterocycles.[16,17]

**2. UV−Visible Absorption and Photoluminescence Spectroscopy.** The UV absorption spectra for compounds **I** and **IIb** in chloroform solutions are presented in Figure 1. Compound **I** exhibits a unique intense absorption peak at 280 nm while compound **IIb** has two intense peaks at 235 and 345 nm and three small peaks at 270, 280, and 290 nm. Their $\lambda_{max}$ show a bathochromic shift of 65 nm as the chemical nature of the pyridine moiety is altered to pyridinium, that is, from 280 nm for **I** to 345 nm for the **IIb**.

The emission fluorescence spectra of both compounds are given in Figure 2. All spectra were recorded from a dilute chloroform solution at $\lambda_{exc.} = 340$ nm for **I** and 380 nm for **IIb** (both values of $\lambda_{exc.}$ were obtained from their excitation spectra). Both compounds exhibit strong emission fluorescence with two maxima at 420 and 460 nm for **I** and 440 and 460 nm for **IIb**.

(16) Baldwin, J. E.; Au, A.; Christie, M.; Haber, S. B.; Hesson, D. *J. Am. Chem. Soc.* **1975**, *97*, 5957.

(17) Leusen, A. M.; Bouna, R. J.; Possel, O. *Tetrahedron Lett.* **1975**, 3487.

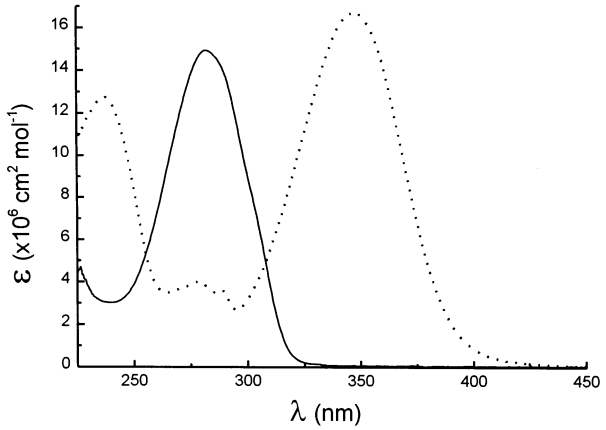


**Figure 1.** UV−visible spectra of compounds **I** (−) and **IIb** (···).

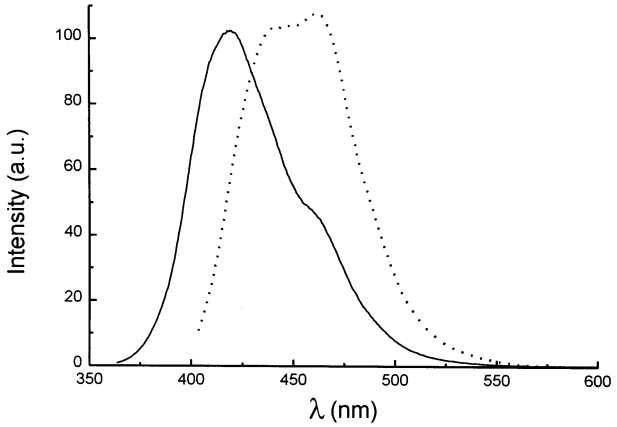


**Figure 2.** Fluorescence spectra of compounds **I** (−) and **IIb** (···).

**3. Mesomorphic Properties.** The thermal stability of the compounds was studied by thermogravimetry (TGA). It was found that all compounds start degrading slightly at temperatures above 140 °C. Severe decomposition becomes evident at temperatures above 170−180 °C, that is, above the clearing temperatures of the compounds (see below). For this reason most of the experiments, especially X-ray diffraction measurements, were performed at temperatures lower than 140 °C. The thermal transitions of the compounds were studied by polarizing optical microscopy and DSC. On heating, they exhibit a crystal−crystal transition at temperatures between 64 and 84 °C depending on the alkyl chain length. On further heating, the compounds melt into birefringent fluid phases at temperatures between 115 and 117 °C. The liquid-crystalline textures observed suggest the presence of a disordered smectic phase. At high temperatures the compounds become isotropic and they simultaneously degrade, as it is very commonly observed for ionic liquid crystals,[18−20] thus preventing the observation of well-developed textures upon cooling. The entropies of the transitions as determined by DSC are reported in Table 1. It becomes evident that the temperature and entropy of the crystal−crystal transition is strongly dependent on the length of the side chains, suggesting that this transition is basically related to the melting of the aliphatic chains. The second crystal−smectic transition is only slightly dependent on their length and is therefore related to the melting of the three-dimensional packing of the oxadiazole−pyridinium bromide cores, leading to the formation of a disordered mesophase.

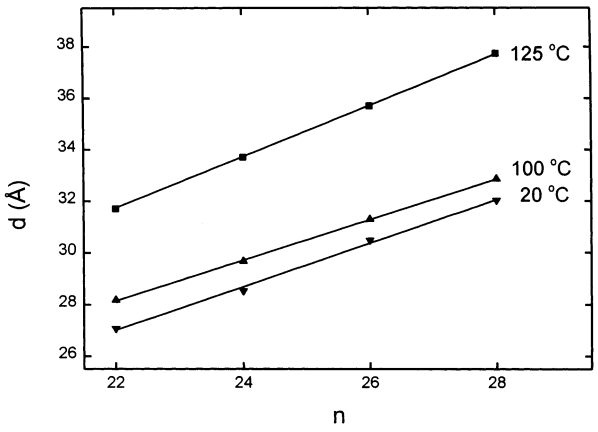


**Figure 3.** Evolution of the lamellar periods *d* as a function of the number of carbon atoms in the aliphatic chains *n* in the $K_1$ (20 °C), $K_2$ (100 °C), and SmA (125 °C) phases.

**Table 1. Transition Temperatures *T* (°C) and Entropies Δ*S* (J·mol$^{-1}$·K$^{-1}$) Observed by DSC**

| compound | *T* [Δ*S*] $K_1-K_2$ | *T* [Δ*S*] $K_2$−SmA | *T* [Δ*S*] SmA−I |
|---|---|---|---|
| **IIa** [$C_{10}$] | 63.9 [94.1] | 117.3 [56.6] | 171.9 [4.2] |
| **IIb** [$C_{12}$] | 73.8 [102.6] | 118.6 [58.3] | 184.6 [4.7] |
| **IIc** [$C_{14}$] | 70.15 [111.7] | 117.6 [61.1] | 186.0 [4.2] |
| **IId** [$C_{16}$] | 84.9 [137.1] | 114.8 [65.8] | 189.1 [3.7] |

The polymorphic behavior observed by POM and DSC was confirmed by X-ray diffraction experiments. The X-ray patterns of the first crystalline phase contain a large number of sharp wide-angle reflections, indicative of a well-developed three-dimensional structure. In the small-angle region more than four equidistant reflections indicate the lamellar ordering of the molecules. The lamellar periods *d* vary linearly with the number of carbon atoms in the aliphatic chains *n*, following the equation $d(\text{Å}) = 8.5 + 0.84n$ ($R = 0.999$), deduced from a least-squares fit of the experimental data (see Figure 3). The *Y*-intercept of the straight line provides an estimate of the thickness of the polar sublayer and it is in agreement with the length of the thioether−oxadiazole−pyridinium bromide group of about 8.2 Å, as estimated using CS Chem3D Pro (Cambridge Soft Corporation). The slope of the *d* versus *n* line (1.68 Å per ethylene unit) representing the length of an ethylene group is less than that in a fully extended paraffin chain (2.54 Å), clearly suggesting that the alkyl chains are interdigitated and tilted with respect to the layer normal. The tilt angle estimated from the experimental data, $\cos^{-1}(1.68/2.54)$, is about 49°. In the second crystalline phase up to five equidistant reflections were observed in the small-angle region. In the wide-angle region the patterns contained a diffuse band indicative of the disorder conformation of alkyl chains together with a number of sharp reflections attributed to the three-dimensional packing of the polar part of the molecules. The lamellar periods grow linearly with *n* according to the equation $d(\text{Å}) = 9.5 + 1.01n$ ($R = 0.999$)

(18) Alami, E.; Levi, H.; Zana, R.; Skoulios, A. *Langmuir* **1993**, *9*, 940.
(19) Tittarelli, F.; Masson, P.; Skoulios, A. *Liq. Cryst.* **1997**, *22*, 721.
(20) Arkas, M.; Paleos, C. M.; Skoulios, A. *Liq. Cryst.* **1997**, *22*, 735.

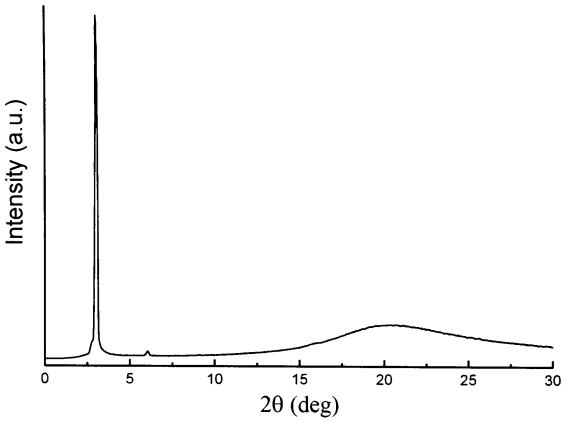


**Figure 4.** X-ray diffraction pattern of compound **IIb** in the SmA phase at 125 °C.

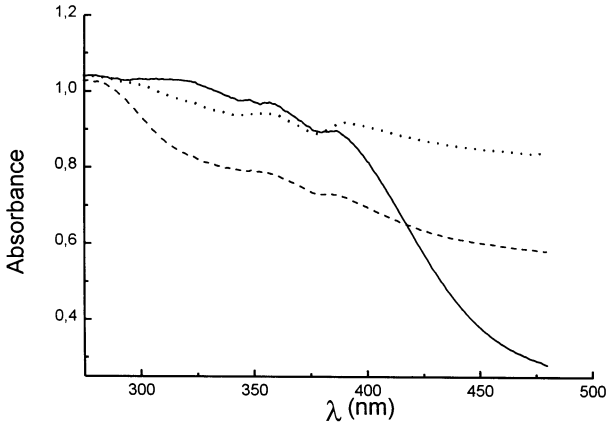


**Figure 5.** UV−visible spectra of compound **IIb** obtained in the solid state at room temperature (···), at 150 °C (—), and upon cooling at 90 °C (- - -) in a quartz cell.

at 100 °C. The increase of the slope of the line simply reflects the volume increase of the alkyl chains upon melting while the *Y*-intercept value obtained—about 1 Å larger that that in the $K_1$ crystal phase—could simply suggest a change in the packing of the oxadiazole−pyridinium group.

At temperatures above the crystal−smectic transitions, the X-ray diffraction patterns contain three sharp equidistant small-angle reflections related to the smectic ordering and a diffuse wide-angle reflection centered at about 4.2 Å, characteristic of the correlation distances between adjacent chains in the disordered conformation (see Figure 4). The smectic periods, deduced from the (001) Bragg reflections, decrease with increasing temperature, as commonly observed in SmA phases, with a relative thermal expansion coefficient $(\partial d/\partial T)/d$ ranging from 4 to $6 \times 10^{-3}$ $K^{-1}$. They also vary linearly with $n$ following the equation $d(\text{Å}) = 10.9 + 0.78n$ ($R = 0.9998$) at 125 °C. The increase of the thickness of the polar sublayer is very commonly observed in amphiphilic-type liquid crystals and can be easily justified due to the fact that the polar groups in the smectic layers are in a more disordered state. However, the substantial decrease of the slope of the $d$ vs $n$ straight line, which is a measure of the distance between two carbon atoms in the aliphatic chain, is rather unusual. Due to the volume expansion of the aliphatic chains, one would expect an increase of this value. Instead, the decrease of this value gives rise to lamellar periods in the smectic phase, which is less than those in the $K_2$ crystal phase and almost equal to the ones of the $K_1$ crystal phase (see Figure 3).

A better understanding of this behavior can be obtained by estimating the molecular area $S$, that is, the area covered by each molecule in the layers. Utilizing the linear dependence of the smectic period on the number of aliphatic carbon atoms and with the reasonable assumption of additivity of the partial volumes of the polar and apolar parts, the molecular area can be calculated from the measured slope (slope $= V_{CH2}/S$) and the volume of one methylene group ($V_{CH2} = 28$ Å$^3$ at 100 °C and 28.5 Å$^3$ at 125 °C).[21] In the $K_2$ crystal phase the molecular area found is 27.7 Å$^2$, while in the SmA phase the area increases by as much as 32% to a value of 36.5 Å$^2$. The melted aliphatic chains extend to fill the molecular area and as a result the thickness of the lipophilic sublayer is decreased. This substantial increase of the molecular area imposed by the polar parts can be rationalized from the fact that the thioether−oxadiazole−pyridinium group cannot be considered as a linear rigid-rod type group. In the SmA phase, where free rotation of the polar part is expected, the effect of the shape caused by the large exocyclic bond angle (of about 134° [22]) forces the groups to occupy more space in the smectic phase, leading to the high molecular area increase observed.

**4. Thermochromic Properties.** The crystal to smectic A transition temperature is also associated with a change in color of the compounds studied: their color changed from pale yellow at room temperature to bright red at high temperatures. This change occurred rapidly right after the transition to the SmA and was almost fully reversible upon cooling, the compounds slowly reverting to yellow. This behavior is certainly not comparable to the darkening observed for some organic compounds upon melting. This thermochromic effect has been studied as a function of the temperature by UV−visible spectroscopy (see Figure 5). At room temperature, the UV spectrum corresponds to the pale yellow/yellow color observed at room temperature, as the compound absorbs almost uniformly all wavelengths in the visible light domain. The spectrum at 150 °C corresponds to the bright red color observed in the mesophase, as it does not absorb above 450 nm. On cooling after crystallization (90 °C), the spectrum shows the progressive return to its initial form. No significant differences have been noted between absorption spectra made at room temperature before and after the heating/cooling cycle.

It should be noted in the first place that the thermochromism of 1-alkyl-4-[5-(dodecylsulfanyl)-1,3,4-oxadiazol-2-yl]pyridinium bromide derivatives is not surprising since compounds bearing the oxadiazole moiety (e.g., polyoxadiazole[23]) or pyridinium salts (e.g., poly(xylyl viologen)s[24]) have been reported to exhibit such properties. For polyoxadiazole, the change in color is generally

(21) Guillon, D.; Skoulios, A.; Benattar, J. J. *J. Phys.* **1986**, *47*, 133.

(22) Lai, C. K.; Ke, Y.-C.; Su, J.-C.; Li, C.-S.; Li, W.-R. *Liq. Cryst.* **2002**, *29*, 915.

(23) Thunemann, A. F.; Janietz, S.; Anlauf, S.; Wedel, A. *J. Mater. Chem.* **2000**, *10*, 2652.

(24) Moore, J. S.; Stupp, S. I. *Macromolecules* **1986**, *19*, 1815.

attributed to a change in the average conjugation distances due to a change in conformation of the main chain. However, it is difficult to accept that such an explanation could apply in the case of small molecules such as the compounds under investigation.

In the case of poly(xylyl viologens), the change of color was attributed to modifications in the level of surface hydration, probably as a result of how water molecules bound to the polymeric ion affect the charge-transfer states between the pyridinium ring and their halide counterion. However, in our case, the change of color cannot be explained in a similar manner since it occurs very quickly, at different temperatures for the different compounds, and is always observed at the transition to the SmA mesophase. It may be more easily understood as the formation/destruction of the colored charge-transfer complex.

It is well-documented that monomeric compounds bearing pyridinium or bipyridinium units, acting as electron acceptors, can form colored charge-transfer complexes with halide ions, acting as electron donors.[25−27] On this basis, the appearance of red color at the crystal to SmA transition can be attributed to analogous charge-transfer interactions. Such interaction cannot take place in the crystalline phases possibly due to the relative positions of the two ions: in the crystalline phase the counterions are expected to be highly localized on the positive charge while close approach of the counterion to the electrophilic aromatic nucleus is needed for strong interaction to occur.[20] In the SmA phase the substantial increase of the molecular area observed can certainly allow the repositioning of the bromine ion closer to the pyridinium nucleus. In this context it should be mentioned that for the poly(xylyl viologens) derivatives it has been suggested that strong interactions occur in amorphous regions. Upon cooling, the slow transition from red to yellow can be explained by the progressive disappearance of the charge-transfer complex trapped in the crystalline phases.

This explanation is furthermore in good agreement with the observations reported some years ago for a mesomorphic *N*-alkylcyanopyridinium derivative. The compound underwent a color change from yellow to red upon entering an ordered smectic B mesophase.[28] X-ray diffraction studies led to the conclusion that its particular molecular organization could be only explained by charge-transfer between the pyridinium moiety and the iodide anion, accounting also for the observed change of color.

## Conclusion

Liquid-crystalline compounds bearing both an oxadiazole and a pyridinium group were synthesized. They have proven able to emit light (good fluorescence properties) and to give rise to disordered SmA mesophases. The materials also exhibited thermochromic properties, their color changing from yellow at room temperature to bright red in the mesophase. It is suggested that this color change can be explained by the formation of a charge-transfer complex in the liquid-crystalline phase. Furthermore, the lamellar organization found in all phases permit a better packing of the aromatic cores that could result in improved electronic properties. Potential applications for these compounds, such as optoelectronic applications or even nonlinear optical generation properties, are of interest and will be examined.

**Acknowledgment.** The authors want to thank Drs. C. Paleos and P. Falaras for fruitful discussions and Dr. Z. Sideratou for technical assistance. D. Haristoy wishes to thank the European Community Marie Curie Fellowship that supported this research.

CM021365G

(25) Kosower, E. M.; Klinedinst, P. E. *J. Am. Chem. Soc.* **1956**, *78*, 3493.
(26) Kosower, E. M. *J. Am. Chem. Soc.* **1958**, *80*, 3253.
(27) Mackay, R. A.; Landolph, J. R.; Poziomek, E. J. *Am. Chem. Soc.* **1971**, *93*, 5026.
(28) Bazuin, C. G.; Guillon, D.; Skoulios, A.; Zana, R. *J. Phys.* **1986**, *47*, 927.